"Reinforcing nodes or wide bridges? How network topology and seeding strategies shape adoption cascades in peer-influence models of complex contagion"

Bart de Bruin [1*], George van Voorn [2], Floor Alkemade [1]

1 Department of Industrial Engineering and Innovation Sciences, Eindhoven University of Technology, The Netherlands
2 Mathematical and Statistical Methods group - Biometris, Wageningen University & Research, The Netherlands

* b.de.bruin@tue.nl

Abstract

Behavioural adoption processes are central to accelerating sustainable transitions. Substantial uncertainty remains regarding how network topology and seeding strategies jointly shape diffusion outcomes. To address this uncertainty, we have developed the Testing Network Topologies And Seeding Strategies (TENTASS) model to test the sensitivity of adoption outcomes to network topology and seeding strategy under conditions of peer influence. Through a systematic full factorial analysis, we demonstrate that the final adoption rate peaks based on the optimum between the required reinforcing nodes around the initial innovators and the wide bridging connections between local neighborhoods. The results show how this optimum shifts due to variations in seeding-related (e.g. innovator density), decision-making-related (e.g. threshold values), and network-related components (e.g. clustering, communities, degree variance). Moreover, the simulations indicate that networks with high variance in node degree or communities can flatten, reverse, or mask the optimum. Lastly, that the effectiveness of seeding strategies highly vary due to structural variation in network topologies. Based on our findings, we argue that the analysis of any network models of transitions should consider the structural uncertainty around the network topology and seeding strategies. Especially given the uncertainty in the structure of real-world peer-influence networks, sensitivity analysis requires mapping how the final adoption rate shifts across a multidimensional parameter space.

1 Introduction

Behaviour change is a key element of the much-needed acceleration of the energy transition. The surging literature on social tipping, the nonlinear processes of transformative change in social systems [1], theorises that especially individual behaviour change plays a crucial role [2]. Specifically, a growing body of evidence points to peer influence as one of the most important accelerators of individual behaviour change in the energy transition [3, 4]. Understanding what drives this kind of rapid, nonlinear diffusion is, therefore, a requirement for effective policy design.

Decisions about whether to adopt solar panels [5], electric cars [6], or energy conservation practices [7–9] are shaped not only by personal circumstances such as income or information access, but also by the behaviour of people in one's social environment [9]. Research on community energy initiatives suggests that indeed people's willingness to participate is strongly determined by whether they have a direct social connection with one of the initiators [10]. The recognition of the importance of behaviour has led to a call in demand-side climate modelling to endogenously integrate social tipping dynamics within larger integrated assessment models, as these fail to capture behavioural heterogeneity, social influence, and non-linear transitions [11].

We argue that current efforts to do so insufficiently take into account the uncertainty associated with real-world social networks, and that this undermines the policy relevance of such modelling efforts. Determining the exact topology of peer-influence networks in the real world based on observational interactions is highly uncertain. Empirical sociological research shows that people frequently communicate without being influenced and that most ties carry little or no persuasive effect [12,13]. Whether such interaction translates into actual behavioural change depends on specific relational and contextual conditions rather than contact alone [14]. Moreover, people are often unable to accurately report who influences their behaviour [15], and empirical network data are known to suffer from substantial measurement errors, including unobserved or omitted connections, misreported connection strengths, and incorrectly aggregated nodes [16,17]. Although empirically observed networks might provide an indication of the actual underlying influence structure, uncertainties about the actual topology of the social network will always remain.

Computational methods, of which agent-based modelling in particular, offers a tool to make this uncertainty explicit and quantifiable. Rather than depending on a single empirical network, agent-based modelling allows researchers to systematically test how sensitive adoption dynamics are to variation in network structure across a wide range of plausible configurations. However, existing modelling studies [18–22] that use agent-based models to evaluate policies to accelerate sustainable transitions make surprising limited use of their evaluative power [23, 24]. Reviews of the literature on such modelling studies show that most agent-based models test the robustness of modelling outcomes for only two or three stylised topologies and produce inconclusive results [23, 24]. In some models, adoption is more widespread in scale-free networks than in small-world networks [25], while in others the topology appears to have only a limited effect on the spread of behaviour [26]. The core problem is that within these studies the sensitivity of the modelling outcome to network topology is only scrutinized by testing two or three very distinct network topologies. This is problematic because network science literature articulates that structural balance between local reinforcement and long-range connectivity [27–31].The generating algorithms cover only a narrow segment of the clustering and degree variance space, while empirical networks like Add Health confound these properties rather than controlling for them independently (see Figure 1). A sensitivity analysis restricted to two or three stylised topologies, or confined to a narrow region of the parameter space, cannot detect how adoption dynamics shift across the full range of plausible network configurations.

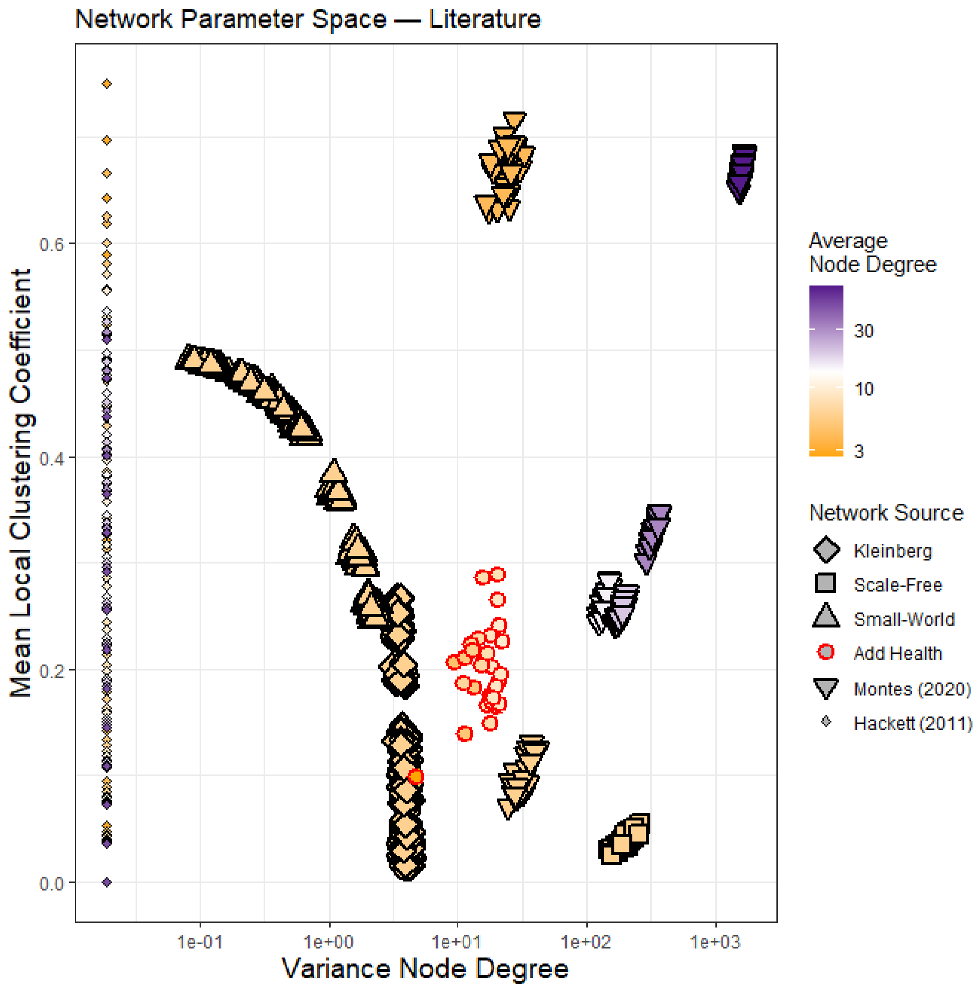

Fig 1. Parameter space coverage of the most widely used network-generating algorithms (Kleinberg, Small-World, Scale-Free) alongside empirical Add Health networks [29] and the simulated networks of Montes et al. [32]. The generating algorithms control for average node degree but trace only a narrow trajectory through the clustering and degree variance space. The Add Health and Montes networks explore a wider range of clustering but do not control for average node degree; moreover, the Montes networks are confined to a high-variance strip due to the preferential attachment mechanism of the Holme-Kim algorithm. Add Health networks are originally directional and have been converted to undirected graphs following Guilbeault & Centola [29]. The data points of the model used by Hackett et al. represent k-regular networks, in which every node has identical degree ($k \in \{3, 4, 5, 6, 8, 10, 15, 20, 30, 50\}$) and variance in node degree is therefore zero by definition [33]. For the the Network generating algorithms we used three of the implemented algorithms within the Netlogo Network Extension library. To compare the algorithims we tried to control for the total number of nodes and connections as much as the algorithm allow for (840 nodes and 5028 nodes for scale-free algorithm, small world and 840 and 5040 links for scale-free algorithm and 841 nodes and 5044 connections for Kleinberg algorithm). For the small-world algorithm by Wattz-Strogratz the rewiring probability we used: 0.01, 0.02, 0.03, 0.04, 0.05, 0.10, 0.15, and 0.20. For the Kleinberg algorithm the clustering exponent we used: 1, 1.2, 1.4, 1.6, 1.8, 2.0, 2.2, 2.4, 2.6, 3, 4, 5, 6). The networks for Singh et al. and Badham et al. are not included in the figure as the variance in node degree could not retrieved based on the available data.

With this paper we therefore ask: *'How is the final adoption rate sensitive to seeding-related (e.g. innovator density), decision-making-related (e.g. threshold values), and network-related components (e.g. clustering, degree variance, communities) within a peer-influence model?'*. To address this research question, we have developed the Testing Network Topology and Seeding Strategies (TENTASS) model. TENTASS is an agent-based simulation built around a new network-generating algorithm that independently controls local clustering, variance in node degree, and average node degree as continuous variables. With this paper, our aim is to make a methodological contribution to prospective ABM-based policy modelling by demonstrating where and why sensitivity to network topology occurs and by proposing a structured approach to sensitivity analysis that researchers can apply when embedding peer-influence networks in larger policy models. The paper continues with a theoretical background on the mechanisms of complex contagion and a review of existing studies on network topologies and adoption rates, followed by the model description, experimental design, results, discussion, and conclusion.

2 Theoretical Background

2.1 Mechanisms of complex contagion

In network science literature, the relationship between final adoption rates, network topology, and seeding strategies has been extensively explored through threshold models of both simple and complex contagion [29–31, 34–36]. Simple contagion follows the logic of infectious disease models: a single exposure to an adopting neighbour can be sufficient to trigger adoption [30]. Under simple contagion, networks with low clustering and many random long-range links tend to accelerate spread because they maximise the number of independent contacts and minimise the average path length. Complex contagion, on the other hand, requires multiple reinforcing signals from different neighbours before adoption occurs [37]. The present paper focuses on complex contagion, as the adoption of sustainable behaviours and technologies involves social reinforcement mechanisms (e.g., peer visibility, social norms, and risk reduction through observation of others) that go beyond the single-exposure logic of simple contagion [28].

To understand the role of network structure under complex contagion, it is important to distinguish three interrelated mechanisms: 1) critical mass, 2) reinforcing nodes, and 3) wide bridges. Critical mass refers to the minimum number of adopters required around a non-adopter such that enough reinforcing signals accumulate to push that person over their adoption threshold [27, 30]. This concept operates at two distinct spatial scales. At the local scale, critical mass determines whether an initial cluster of innovators can trigger adoption among their immediate neighbours, causing a local cascade. On the global scale, it determines whether this local cascade can bridge across to other parts of the network and sustain itself beyond the initial neighbourhood, converting a local cascade into a global one [30, 38].

On the local scale, critical mass is reached through *reinforcing nodes*, neighbours of a target individual who are also connected to each other, meaning that the same adoption signal reaches the target through multiple independent pathways rather than just one [28, 29]. Local clustering, the extent to which an individual's neighbours are also connected to one another, is the network metric that captures this density of reinforcing nodes [37, 39].

At the global scale, the transition from a local cascade to a global one depends on *wide bridges*, connections between two different neighbourhoods that are themselves reinforced by at least one other set of connected neighbours who each are part of one of the two neighbourhoods [28, 29]. Under simple contagion, a single connection between two neighbourhoods is sufficient to carry an adoption signal across the boundary [27]. Under complex contagion however, a single unreinforced connection cannot provide sufficient signals to trigger adoption in the receiving neighbourhood. Wide bridges solve this problem by providing cross-neighbourhood connections that are backed by multiple reinforcing nodes [28, 29].

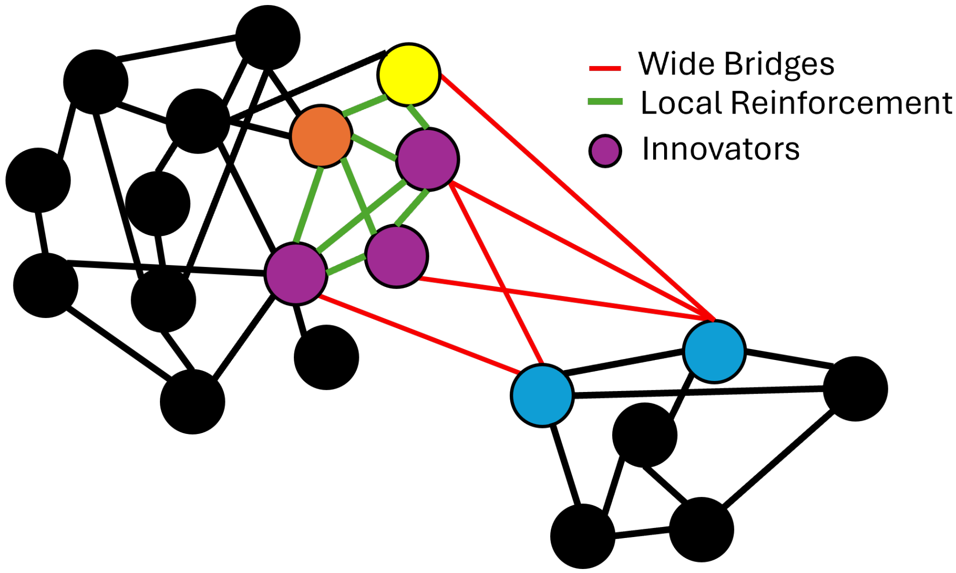

Fig 2. Illustration of Local Reinforcement and Wide bridges. In this example the orange node will adopt due to being connected with three innovators. The adoption of the orange node than initiates a local cascade as the local reinforcement causes the yellow node also to adopt. This local cascade might cause a global cascade when there are enough wide bridges between the two neighbourhoods that make the blue nodes to adopt as well.

This distinction between reinforcing nodes and wide bridges reveals a fundamental tension within complex contagion. High local clustering generates more reinforcing nodes within neighbourhoods, facilitating local adoption cascades. However, high clustering simultaneously reduces the number of wide bridges available between neighbourhoods, because connections become increasingly concentrated within the same local cluster rather than reaching across to other parts of the network [27, 40, 41]. Highly clustered networks are therefore effective in sustaining local cascades but poor in enabling those cascades to become global. Second, the network-generating algorithm must be able to vary the balance between local clustering and wide bridges independently of other structural properties, so that the contribution of each can be isolated

2.2 Prior work on network structure and adoption outcomes

The fundamental tension between reinforcing nodes and wide bridges has motivated a body of work aimed at understanding how specific structural properties shape adoption outcomes under complex contagion. Singh et al. [31] demonstrate that when average node degree is held constant, higher local clustering produces higher final adoption rates under complex threshold-based contagion, confirming the importance of reinforcing nodes for reaching local critical mass. This finding establishes clustering as a primary structural driver of adoption but only under controlled conditions where other structural properties are fixed.

Hackett et al. [33] extend these findings by showing that the effect of clustering is not monotonic: depending on average node degree, higher clustering can either increase or decrease final adoption rates. However, Hackett et al. achieve this analytical clarity only by assuming a homogeneous node degree distribution in which every node has identical degree. Badham et al. [35] explicitly identify this assumption of homogeneous node degree distribution as empirically unrealistic. Relaxing this assumption and allowing clustering, average node degree, and degree variance to vary simultaneously, Badham et al. find that structural properties produce strong but context-dependent and sometimes contradictory effects on diffusion, which they attribute to confounding co-variation between structural components [35].

The relationship between clustering and adoption is further complicated by where innovators are placed within the network. Guilbeault & Centola [29] introduce a topological measure, called complex closeness centrality, that weights shortest paths by the reinforcing influence of shared connections between nodes(see Figure 6). They demonstrate that this measure predicts the spread of complex contagion better than standard centrality measures such as degree or betweenness, and that seeding strategies based on complex closeness centrality outperform degree-based seeding across empirical Add Health networks. Their findings confirm that the structural position of innovators within the network shapes adoption outcomes under complex contagion. Montes et al. [32] examine seeding strategy effectiveness under a probabilistic contagion mechanism, in which each infected node transmits to susceptible neighbours with a fixed probability rather than requiring a threshold proportion of adopting peers. Under this mechanism, they find that the relative performance of centralised versus decentralised seeding strategies varies depending on network density and clustering coefficient: decentralised strategies outperform in sparse networks with community structure while centralised strategies perform better in denser networks. This suggests that even under probabilistic contagion, where adoption does not require reinforcing signals, the structural properties of the network moderate which seeding strategies are most effective.

Taken together, these findings suggest the existence of an adoption optimum along the clustering dimension. This optimum represents the level of clustering at which the network simultaneously sustains local cascades through reinforcing nodes and enables them to become global through wide bridges. The findings of Hackett et al., Badham et al., Guilbeault & Centola, and Montes et al. further suggest that this optimum shifts depending on average node degree, seeding strategy, and local clustering. How these components jointly displace the optimum across a continuous multidimensional parameter space, and whether properties such as variance in node degree can cause it to disappear entirely, remains unknown.

3 Model Description

The TENTASS model is an agent-based model designed to test the sensitivity of adoption outcomes to network topology and seeding strategy under conditions of peer influence. Within this section we will describe the three core components that are essential for interpreting the results: 1) the decision modules that govern how agents adopt behaviour, 2) the network-generating algorithm and the network topologies it produces, and 3) the variety of seeding strategies that are used to determine the location of social innovators within the network. The model have been implemented in the agent-based modelling software Netlogo 6.4.0. The model code, data analysis and processing files can be found in the supplementary material.

3.1 Decision modules

The model consists of a single type of agent representing people who perform sustainability-related practices in their daily life. Each agent holds a binary behaviour attribute $b \in \{0, 1\}$, where $b = 0$ represents the current behaviour and $b = 1$ the alternative sustainable behaviour. At initialisation, a small share of agents are assigned $b = 1$ as social innovators (see Section 3.3); all others begin with $b = 0$. The decision to adopt is governed entirely by peer influence: all other drivers of behaviour change (transaction costs, learning effects, prior experience) are deliberately excluded so that the sensitivity of adoption outcomes to network structure can be isolated. Two decision modules are implemented, which differ in whether adoption is reversible.

The **threshold module** is the decision rule used in classical diffusion of innovation models [27, 29, 30]. An agent adopts the new behaviour when the fraction of its connected peers who have already adopted exceeds a threshold (ϕ):

ϕ:

$$\Pr(b_t = 1 \mid b_{t-1} = 0) = \frac{F_{b_{t-1}=1}}{F} > \phi \tag{1}$$

where $Pr(...)$ is the probability that an agent switches to behaviour '1' given the agent now exhibits behaviour '0', F is the total number of peers and $F_{b_{t-1}=1}$ is the number of peers who adopted at the previous timestep.

Adoption is assumed to be irreversible: once an agent switches to $b = 1$ it remains there. Simulations run until no further agents switch behavior in a given timestep.

The **probabilistic module** replaces the binary threshold rule with a continuous probability of adoption that is proportional to the fraction of peers currently holding each behaviour:

$$\Pr(b_{t+1} = 1 \mid b_t = 0) = \frac{F_1 + \epsilon 1}{F + \epsilon 2}, \qquad \Pr(b_{t+1} = 0 \mid b_t = 1) = \frac{F_0 + \epsilon 1}{F + \epsilon 2} \tag{2}$$

where F_1 and F_0 are the numbers of peers holding behaviour 1 and 0 respectively, and $\epsilon 1, \epsilon 2 > 0$ are small constants (set to 10^{-6}) that prevent division by zero while keeping stochastic noise negligible. Hence, in the beginning of the simulation when $F_1 \ll F$ the probability of switching to behaviour '1' is small and a local 'hub' of early adopters is required to 'kickstart' the contagion. Adoption is reversible in this module: agents can switch between behaviours at each time step. As a result, it is possible for transitions to stop and even switch back. Simulations are stopped when the total share of adopters either exceeds 95% or drops below 5% of the population.

The two modules represent qualitatively different behavioural assumptions. The threshold module mimics behaviours with high sunk costs or social commitment effects, where adoption is a one-way decision. The probabilistic module captures behaviours that are more easily reversed, such as dietary change or energy conservation practices.

3.2 Network generation

To enable systemic analysis across the parameter dimensions of average local clustering coefficients and node degree variance while controlling for node degree, we introduce the TENTASS model. An overview of all network structural metrics used throughout this paper with their formal definitions is provided in Table 2 in the Appendix. The model is based on five input parameters: mean node degree ($\bar{k}$), number of communities (G), clustering exponent (C), rewiring proportion (R), and Dekker's power (Q). Network formation follows four steps:

- **Step 1.** On initiation, agents receive an unique identity number I which is used for assigning agents to communities and for the clustering coefficient. To distribute agents between communities, they are ranked by identity value and assigned equally to G communities.
- **Step 2.** Each of the G communities has connections to the other communities as well as within-community connections. Within-community connections are added using a Kleinberg-based procedure [42]. The probability that agent x connects to agent y within the same community depends on the clustering exponent C:

$$P(E_{xy} = 1) = \begin{cases} \left(\dfrac{1}{|I_x - I_y|}\right)^C & \text{for } |I_x - I_y| < \dfrac{N}{G \cdot 2} \\ \left(\dfrac{1}{\dfrac{N}{G \cdot 2} \cdot |I_x - I_y|}\right)^C & \text{for } |I_x - I_y| > \dfrac{N}{G \cdot 2} \end{cases} \tag{3}$$

  where $|I_x - I_y|$ is the absolute difference in identity value I between agents x and y. Higher values of C concentrate connections among agents with similar identity values, producing higher local clustering. This step repeats until the user-defined parameter average node degree $\bar{k}$ is reached.
- **Step 3.** To ensure a connected network is established, to allow for heterogeneity in node degree and to create wide bridges a proportion R of connections are rewired between agents irrespective of their community, using the extended Kawachi rewiring process developed by Dekker [43]. The rewiring

procedure is applied three times, giving an effective rewiring probability of $1-(1-R)^3$. The connection between agent x and agent y is replaced by a connection between agent x and agent z, where the probability of selecting z is:

$$P(E_{x,z}=1)=\frac{(k_z+1)^Q}{\sum_{n\neq x}(k_n+1)^Q} \tag{4}$$

where k_z is the node degree of agent z, k_n is the degree of all agents excluding agent x and agents already connected to x, and Q is Dekker's power. Higher R reduces clustering and introduces wide bridges. Combining moderate R with high Q increase the heterogeneity of the average node degree, as hub nodes are created by replicating the preferential attachment dynamic of scale-free networks [44]. A low Q (e.g. 0) results in many rewired connections but no hubs.

- **Step 4.** If the resulting network is disconnected, the full procedure is repeated from scratch until a connected network is obtained.

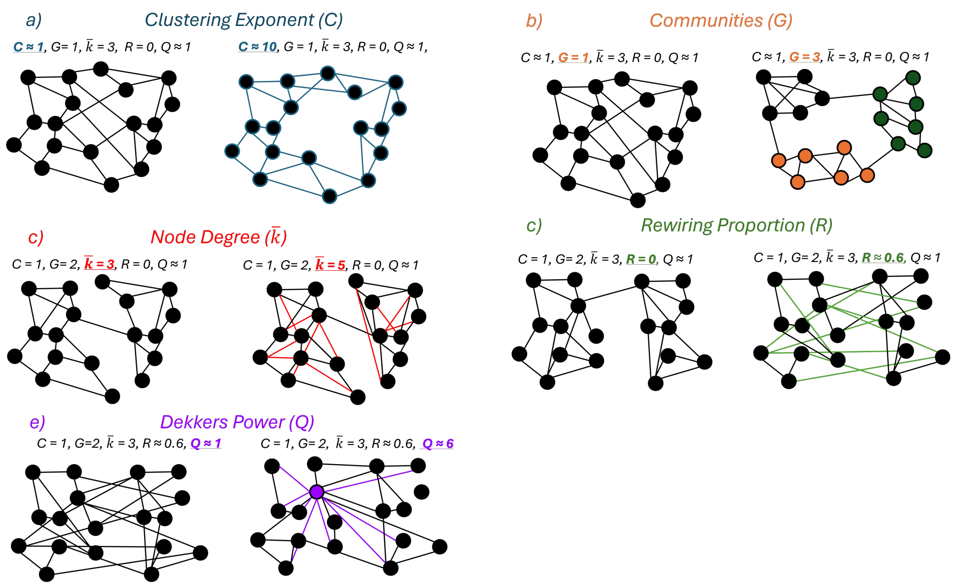

Fig 3. Influence of the network input parameters on resulting network structure configurations.

Figure 3 illustrates the effect of each input parameter on the resulting network structure. Figure 4 shows how, compared to the previous mentioned network generating-algorithms and network studies, the networks generated by TENTASS algorthim cover a substantially wider and more continuous region of the clustering and variance node degree parameter space, while maintaining average node degree as an independent variable.

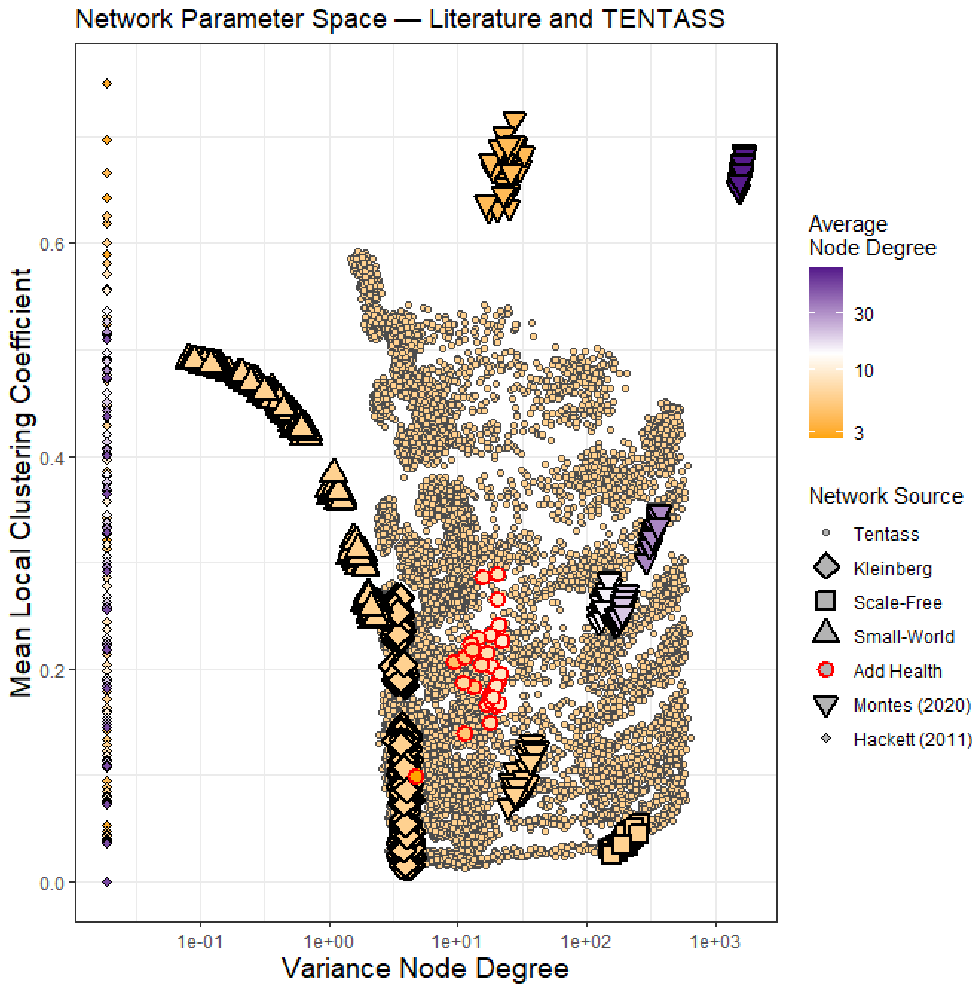

Fig 4. Coverage of the network structural parameter space (mean local clustering coefficient versus variance in node degree) for TENTASS networks generated with average node degree fixed at 6, compared to the Kleinberg, Small-World, and Scale-Free generating algorithms, empirical Add Health networks [29], and simulated Montes et al. networks [32]. TENTASS settings: communities 1, 5, 10; rewiring proportion 0.01, 0.05, 0.1, 0.2; Dekker's power 1, 3, 5, 7; clustering exponent 1, 1.4, 1.8, 2.2, 2.4, 2.6, 2.8, 3, 4, 5, 6; 25 replications per setting. For algorithm comparison settings see Fig 1.

3.2.1 Resulting network structure and correlation analysis

The five input parameters jointly determine the structural properties of the generated networks. To verify that the four primary structural descriptors, variance in node degree (VD), mean local clustering coefficient (MLC), average node degree ($\bar{k}$), and modularity, are sufficiently independent to serve as meaningful axes for sensitivity analysis, we computed a Spearman correlation matrix across all networks generated under the Full Factorial parameter settings described in Section 4 (Fig 5). Within the present design, variance in node degree (VD), mean local clustering coefficient (MLC), average node degree ($\bar{k}$), the variance in the local clustering coefficient (VLC), and modularity a show the lowest mutual correlations and are therefore used as the primary structural descriptors throughout the results section. The mean complex path length (MCPL), the mean path length (MPL) and the global clustering coefficient (GCC) are included in the matrix for completeness, but are not used as primary axes due to their higher correlations with the four selected metrics (see Table 2 in the Appendix for formal definitions of all eight metrics).

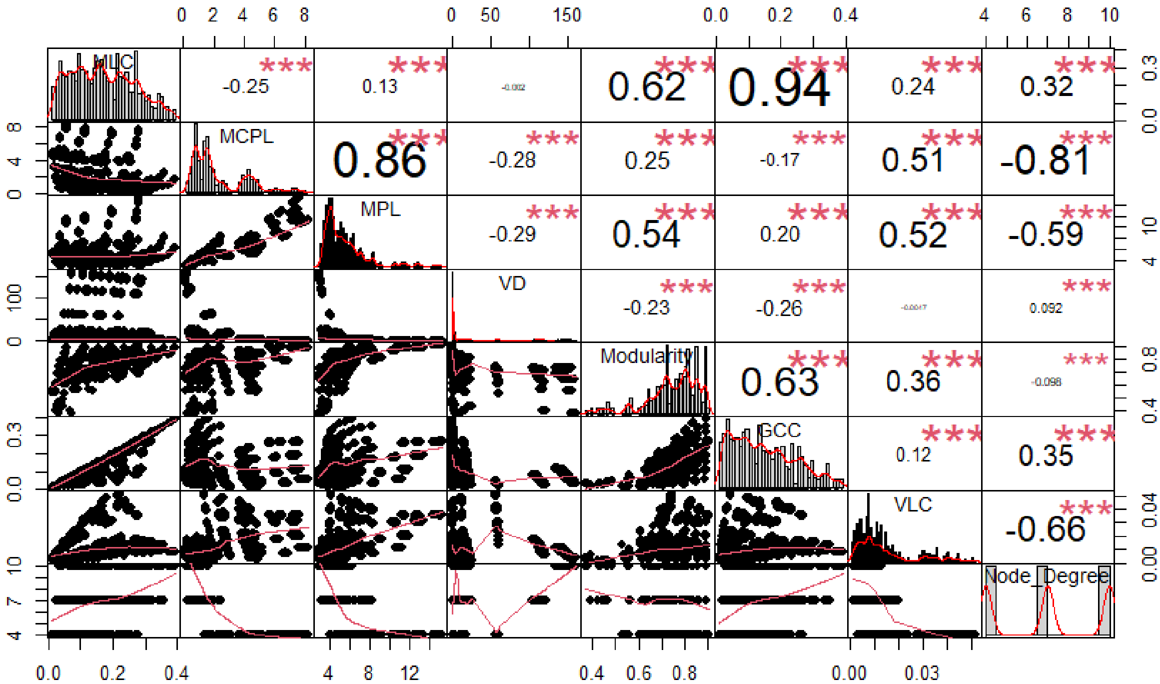

Fig 5. Spearmann correlation matrix between network metrics for all networks generated in the Full Factorial analysis (parameter settings as listed in Table 1). The metrics are mean local clustering coefficient (MLC), mean complex path length (MCPL), mean path length (MPL), variance in node degree (VD), modularity,, and modularity, global clustering coefficient (GCC), and variance in local clustering coefficient (VLC), average node degree (Node_Degree). Formal definitions of all metrics are provided in Table 2. Pink asterisks indicate statistical significance (*** $p < 0.001$).

3.3 Seeding strategies

At initialisation, a proportion of agents are designated as social innovators with $b = 1$; all remaining agents begin with $b = 0$. This proportion is an input-parameter called innovator density (ρ). Three seeding strategies determine which agents are selected as innovators.

- The **Shotgun** strategy assigns innovators randomly. It serves as the baseline against which the effect of targeted seeding strategies can be assessed.
- The **Silver Bullets** strategy selects innovators in descending order of node degree k_i, targeting the most highly connected agents first. Singh et al. [31] showed that this strategy maximises the range of threshold values over which large-scale adoption occurs, because high-degree nodes simultaneously reach many peers and generate a large initial adopter pool.
- The **Snowball** strategy is based on the complex centrality seeding approach introduced by Guilbeault & Centola [29]. A focal node with the highest complex closeness centrality is selected first, followed by its direct neighbours, and then expanded iteratively to the next agent with the highest proportion of

connections already designated as innovators. Complex closeness centrality weights directed shortest paths by the complex edge weight $w_{x \to y}$, which captures the reinforcing influence of shared connections:

$$w_{x \to y} = \frac{1}{1 + o_{xy} + r_{xy}} \tag{5}$$

where o_{xy} is the number of nodes connected to both x and y, and r_{xy} is the number of nodes connected to y but not x that share at least one connection with a neighbour of x (i.e. reinforcing nodes). Even though the connections are unidirectional, the location of reinforcing nodes may cause that $w_{x \to y} \neq w_{y \to x}$ (see Figure 6. The complex closeness centrality of agent x is then:

$$c_x = \frac{1}{\sum_{y \neq x}(w_{x \to y})} \tag{6}$$

Where c_x = the complex closeness centrality of person x, and $w_{x,y}$ the complex weight between person x and person y.

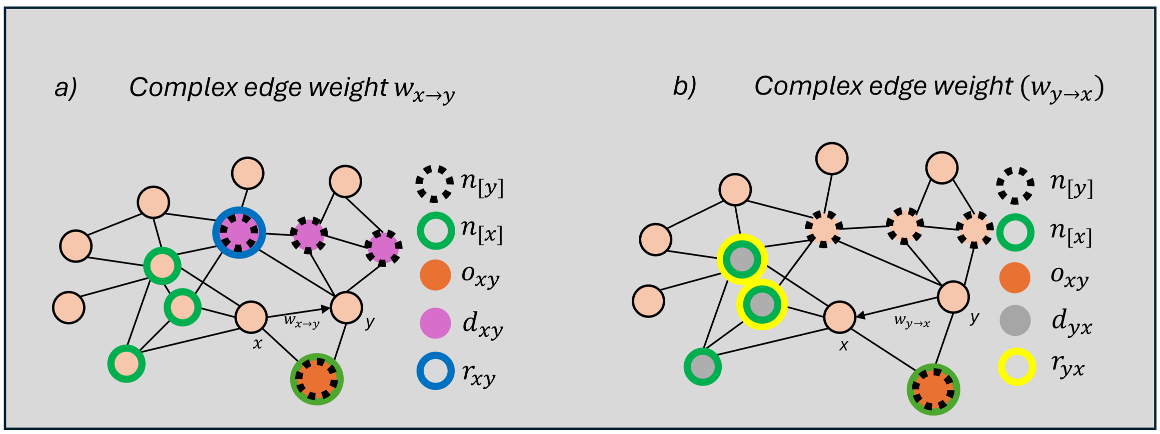

Fig 6. *Example of how reinforcing influences exerts discrepancy between the indirect influence of person x on person y and the indirect influence of persony on person x. The network in the left panel showcases the different sets of nodes that determine the complex weight ($w_{y \to x}$) of the directional connection from person x to person y. Where $n_{[x]}$ is the set of all people besides person y that are connected to person x, resembles $n_{[y]}$ which is the set of all people besides person x that are connected to person y, $o_{[xy]}$ are the set of nodes that are both in $n_{[x]}$ and $n_{[y]}$, $d_{[xy]}$ are all the people that are connected to person y but not to person x, and $r_{[xy]}$ is the subset of $d_{[xy]}$ who are connected to at least one of the nodes in $n_{[x]}$. Within the given example this results that $w_{x \to y} = \frac{1}{1 + o_{xy} + r_{xy}} = \frac{1}{1+1+1} = \frac{1}{3}$. On the contrary, the panel on the right illustrates the node sets that are used to compute the complex weight of ($w_{y \to x}$) which is the influence of person y over person x. Similarly to the left panel, is $n_{[x]}$, and is $o_{[xy]}$. $d_{[yx]}$ are all the people that are connected to person x but not to person y, and $r_{[yx]}$ are the subset of $d_{[yx]}$ that are connected to at least one of the nodes of $n_{[x]}$. Within this given example the $w_{x \to y} > w_{y \to x}$ as*
$w_{y \to x} = \frac{1}{1 + o_{yx} + r_{yx}} = \frac{1}{1+1+2} = \frac{1}{4}$.

The key distinction between the Snowball strategy and the other two seeding strategies is that it produces a spatially concentrated cluster of innovators. The other strategies, Shotgun and Silver Bullets, assign innovators more uniformly across the network (see Figure 7). This concentration means that the Snowball strategy relies more heavily on wide bridges to accelerate towards a global cascade, and therefore interacts differently with network structure than the other two strategies.

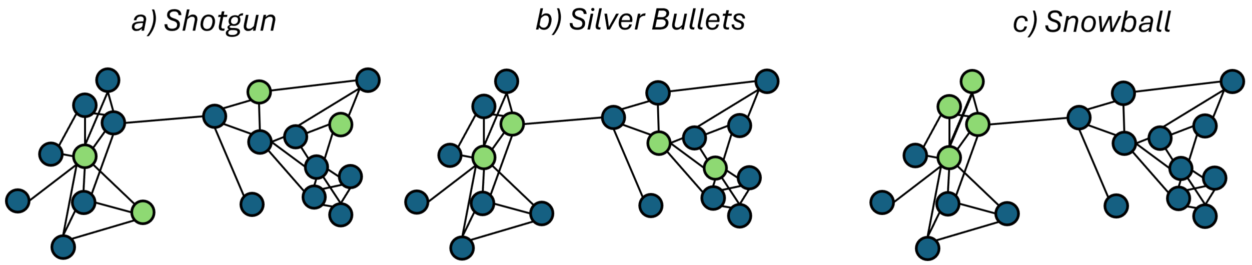

Fig 7. Illustration of the three seeding strategies: a) Shotgun (random assignment), b) Silver Bullets (highest node degree k_i), and c) Snowball (highest complex closeness centrality c_x with outward expansion). Green nodes are social innovators ($b = 1$); blue nodes are non-adopters ($b = 0$).

4 Experimental Design

4.1 Experimental setup

We performed a Full Factorial analysis across the parameter space of the TENTASS to map how adoption outcomes vary across the continuous structural space defined by network metrics. The model parameters vary in three dimensions: i) the network configuration, determined by five input parameters ($\bar{k}$, G, C, R, Q); ii) the decision module and threshold values (Probabilistic, Threshold); and iii) three seeding strategies (Snowball, Shotgun, Silver-Bullets) and innovator density (ρ). The full set of parameter settings are listed in Table 1. Together, these resulted in 31,104 unique parameter combinations. Each combination was repeated 350 times with different random seeds to control for stochasticity in network generation, innovator location, and agent decision-making.

Table 1. Overview of parameter settings used in the Full Factorial analysis.

Symbol	*Netlogo Name*	*Settings*
N	Total-Population	$[840]$
$\bar{k}$	Average-Node-Degree	$[4, 7, 10]$
Q	Dekkers-power	$[1, 3, 5, 7]$
R	Rewiring-probability	$[0.01, 0.05, 0.10, 0.20]$
C	Clustering-Exponent	$[1, 1.4, 1.8, 2.2]$
G	n-communities	$[1, 5, 10]$
S	Seeding-Strategy	$[\text{Shotgun}, \text{Silver Bullets}, \text{Snowball}]$
ρ	Innovator Density	$[0.1, 0.2, 0.3]$
D	Decision-Making-Module	$[\text{Threshold}, \text{Probabilistic}]$
T	Threshold	$[0.3, 0.4, 0.5, 0.6, 0.7]$

The parameter ranges were selected to span the range in which sensitivity of the final adoption rate is observable. For the threshold and innovator density parameters, a very low threshold combined with many

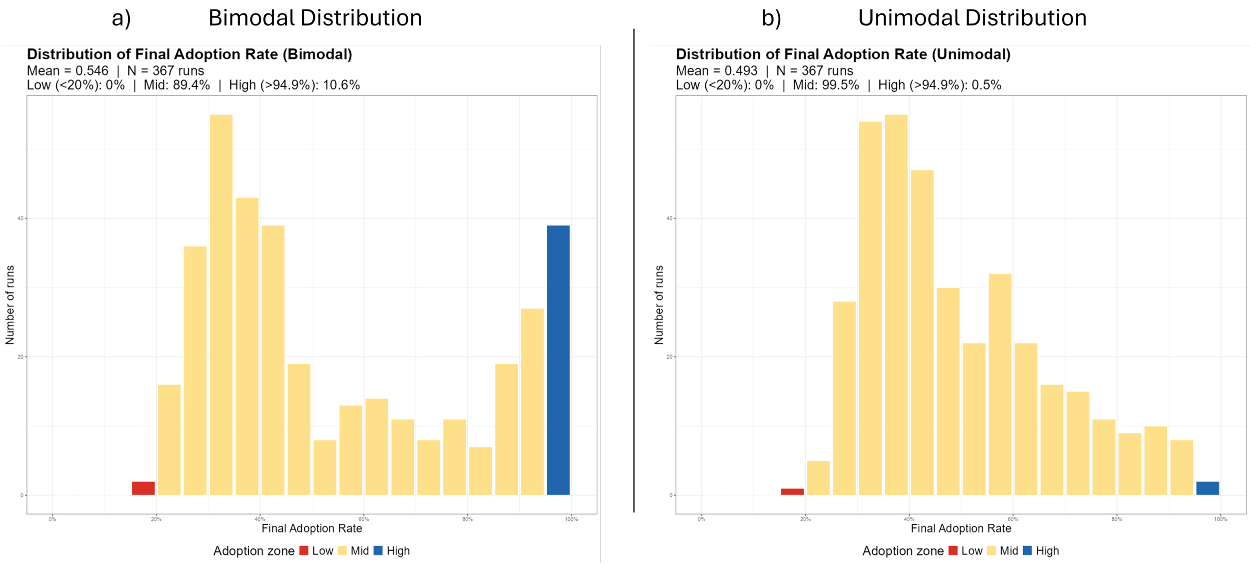

Fig 8. Illustration of how based on the model the configuration the distribution of repetitive runs are either bimodal (panel a) or unimodal (panel b)

innovators, or a very high threshold with very few, produce adoption outcomes that are not sensitive to network structure. Cascades either always occur or never occur regardless of topology. The selected combinations ensure that a meaningful range of adoption outcomes is observable across different network configurations. For the network parameters, the ranges were calibrated to cover as wide a region of the clustering and degree variance space as possible given the model's input parameters; Figure 4 demonstrates that the TENTASS model at these settings covers a substantially wider structural parameter space than existing generating algorithms or empirical networks.

The primary output variable is the *final adoption rate*: the proportion of agents holding $b = 1$ at the end of a simulation run. For the threshold module this is the share of adopters at the timestep when no further adoption occurs; for the probabilistic module it is the share at the timestep when the 95% or 5% stopping condition is met. All results are reported as means across the 350 repetitions per parameter combination. The distribution of repetitive runs are either bimodal distributed or unimodal distributed (see Figure 8. A mean of repetitive runs with bimodal adoption distribution (indicated by a *square* shape) indicates that among the replications in some runs a global cascade occurred and all agents have adopted, while in others the local cascade fails to propagate beyond the innovators. The mean with bimodal distribution should therefore be interpreted as a percentage of runs in which full adoption occurs. An unimodal distribution of repetitive runs indicates that all simulation runs are normally distributed around the mean. Throughout the results, bimodal parameter combinations are indicated by a square marker and unimodal combinations by a circle.

To explore the large and non-linear output space, the full simulation results are made available through an interactive web application that allows users to filter by seeding strategy, decision module, network topology parameters, and innovator density, and to inspect example network visualisations for any selected parameter combination [45].

5 Simulation Results

5.1 Effects of Decision Modules

The first simulation results compares the influence of different conceptualizations and operationalisations of decision-modules to the sensitivity of network structure to the final adoption rate. To showcase this influence, we compared the non-reversible threshold decision module with the reversible probabilistic decision module. When the decision module is set to threshold (Figure 9, panel a), there is a clear distinction between simulation runs in how different network topologies and seeding strategies influence the final adoption rate. When running the model using the probabilistic decision module, the sensitivity of network topologies and seeding strategies to the final adoption rate diminishes (Figure 9, panel b). The reason for this outcome is that within the probabilistic decision module the adoption is reversible (people can continuously switch between the new and old state). For a network with topologies that allow for a wide spread of behavior, temporal oscillations are visible from non-adoption to adoption and back, until a full consensus is reached (either full adoption or full non-adoption). When averaging across simulation runs, the final adoption rate remains largely equal to the initial innovator density. The slight distinction between Silver Bullets and the other two seeding strategies is caused by the fact that within the Silver Bullet strategy, highly connected people are targeted as initial innovators, resulting in a higher probability of adoption taking off. These results indicate that especially for models that are aimed at reversible sustainable behaviours with low sunk investments (e.g. sustainable diets), the final adoption rate for models with an alteration to the default threshold decision-module may be very different in terms of sensitivity to network topology or seeding strategies.

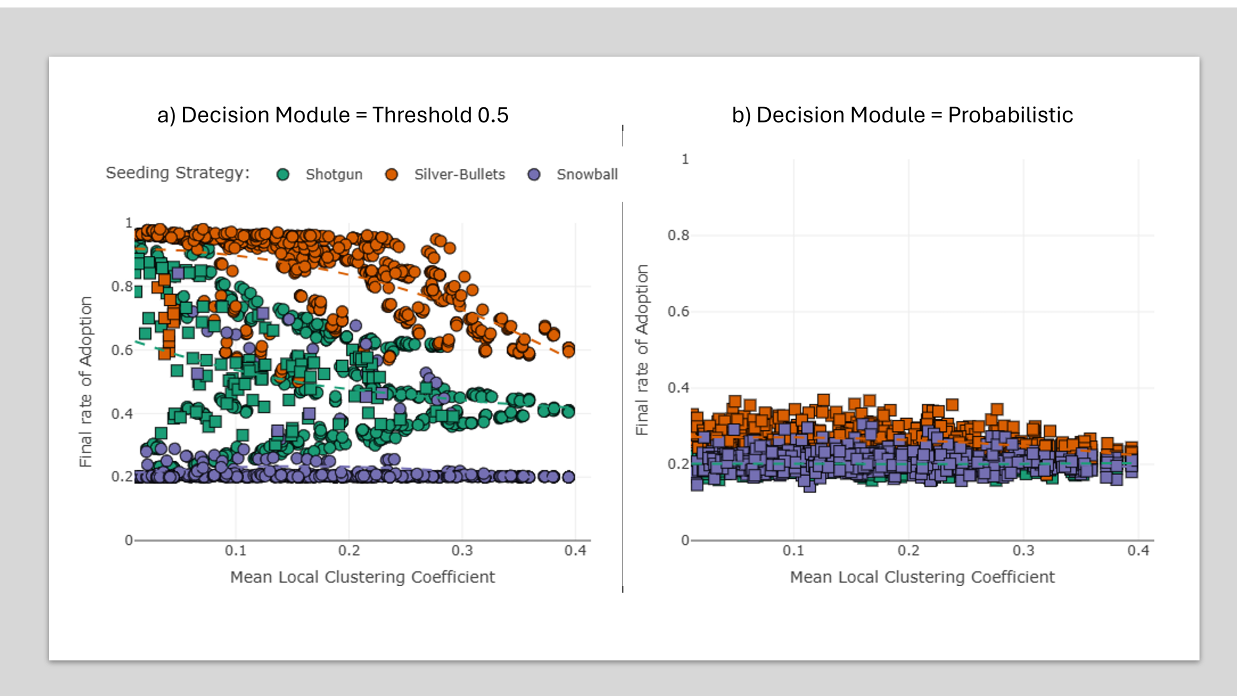

Fig 9. Comparing the two different types of Decision_Modules: Threshold and Probabilistic with the following settings: Decision_Module = Threshold 0.5, Probabilistic, Innovators = 0.2, Seeding_Strategy = All, Node_Degree = All, Communities = All, Dekkers_Power = All, Rewiring_Proportion = All, Clustering_Exponent = All. The round shaped markers indicate that across repetitive runs, the adoption outcome is unimodal distributed. Square shaped markers have a bimodal adoption distribution.

5.2 Effect of Threshold and Innovator Density

Figure 10) shows how the sensitivity of final adoption to network topology is not constant but highly dependent on the specific combination of model parameters chosen.

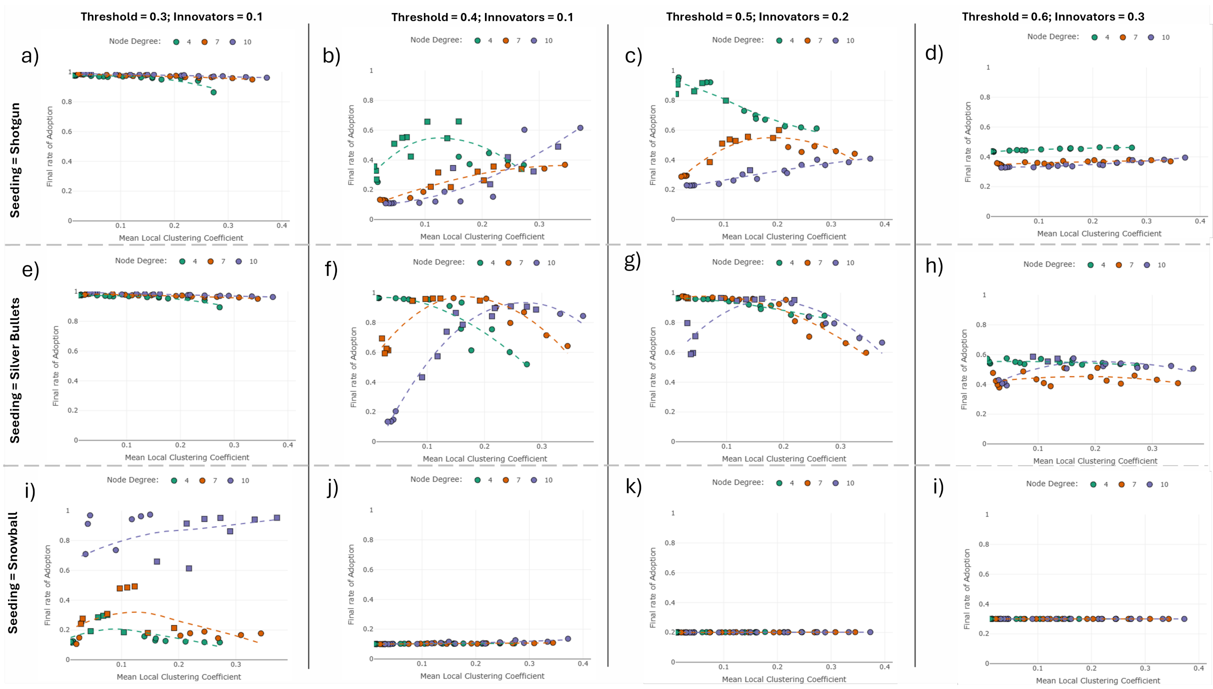

Fig 10. Indication of how the optimum in the final adoption rate (y-axis) shifts for networks with varying average local clustering coefficients (x-axis).For every graph within this figure the networks with the following parameters are included, Dekker's Power = 0; communities = 1; rewiring proportion = 0.01, 0.05, 0.1, 0.2, clustering exponent = 1, 1.4, 1.8, 2.2. The round shaped markers indicate that across repetitive runs, the adoption outcome is unimodal distributed. Square shaped markers have a bimodal adoption distribution.

For the Shotgun (upper row) and Silver Bullets (middle row) seeding strategies, the results reveal that depending on the threshold/innovator combination, the final adoption rate has an optimum along the mean local clustering dimension. In networks with a lower threshold value and fewer innovators, the critical mass at the local scale is easily reached: a small, densely clustered neighbourhood around the initial innovators provides sufficient reinforcing signals to trigger a local cascade. Under these conditions, high clustering is beneficial because it concentrates the limited number of adopting signals around individual non-adopters, making it more likely that any given person accumulates enough peer influence to cross their threshold.

However, high local clustering reduces the probability of triggering a cascade on a global scale. Highly clustered networks have fewer bridging connections that cross between neighbourhoods, meaning that the local cascade remains limited to within the initial cluster of innovators and fails to expand across the whole network. The optimum therefore represents the level of clustering at which the network is most efficient at simultaneously sustaining the local cascade and enabling it to transition into a global one.

A higher threshold means that more reinforcing signals are needed before any individual adopts, requiring a broader base of clustered connections to reliably generate local cascades. On the other hand, a larger innovator density means that more signals are already present to initiate a local cascade reducing the necessity of high clustering with reinforcing nodes. The optimum therefore shifts leftward towards a lower clustering coefficient as this leads to an increase of reach in the network.

For networks with a lower average node degree (e.g. $\bar{k} = 4$), green curves in Figure 10), each individual has fewer connections, meaning the threshold value of adopting peers is reached with fewer absolute adopters. Critical mass at the local scale is therefore reached at a lower absolute level of clustering, shifting the optimum to the left. For higher degree networks (e.g. blue lines in Figure 10), on average more adopting neighbours are needed to surpass the threshold, requiring a higher clustering coefficient to concentrate enough reinforcing signals around any given non-adopter, which pushes the optimum in the rightwards.

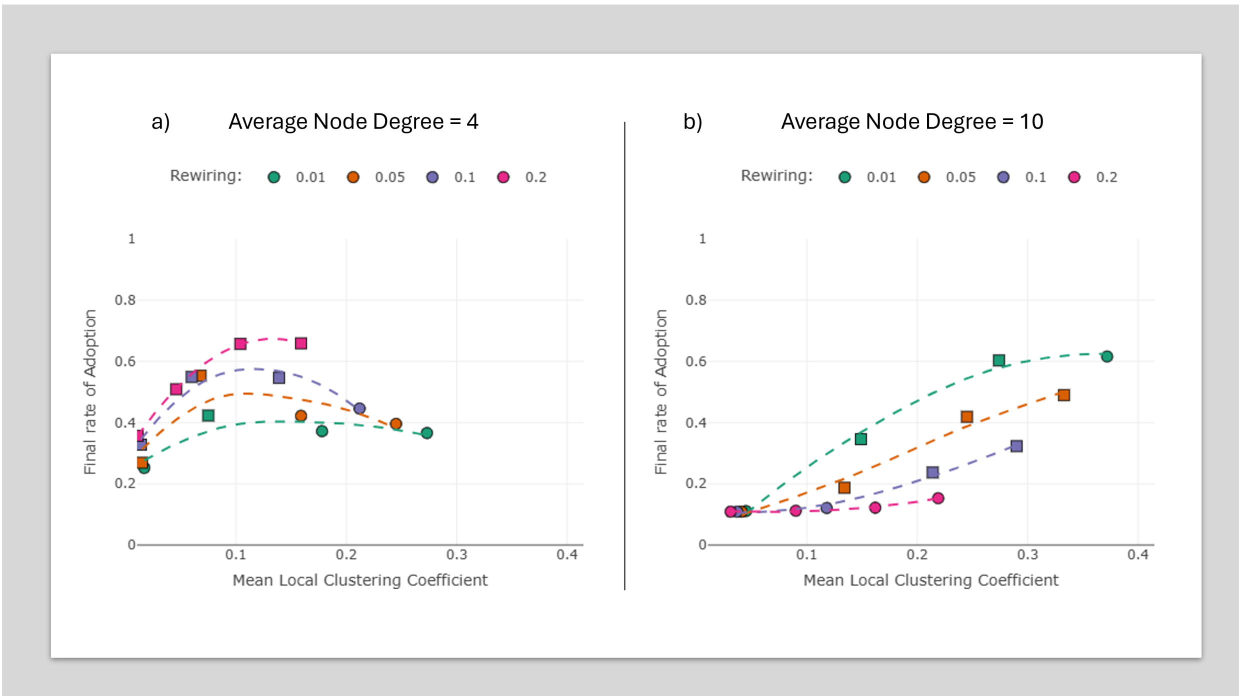

Fig 11. This figure is a specification of graph B from Figure 10. The the following parameters are included, Dekker's Power = 0; communities = 1; rewiring proportion = 0.01, 0.05, 0.1, 0.2, clustering exponent = 1, 1.4, 1.8, 2.2, seeding strategy = shotgun. The Figure shows the sensitivity of having a higher rewiring proportion to the final adoption rate to networks with an average node degree of 4 (left panel) and 10 (right panel). The colors indicate the networks with different rewiring: green = 0.01, orange = 0.05, blue = 0.1, pink = 0.2. The round shaped markers indicate that across repetitive runs, the adoption outcome is unimodal distributed. Square shaped markers have a bimodal adoption distribution.

To further showcase the relationship between node degree, reinforcing nodes and wide bridges we have made a more extensive analysis of graph b from Figure 10. Within Figure 11 We specified the simulations runs further based on the different settings for the rewiring proportion parameter, which for higher settings reduces clustering and introduces long-range bridges between neighbourhoods in the network. For networks with a low average node degree ($\bar{k} = 4$ panel a of Figure 11), very low rewiring ($R = 0.01$) in the network causes it to be too locally clustered to generate sufficient bridging connections for a global cascade. At higher rewiring ($R = 0.02$), the optimal balance between reinforcing nodes and wide bridges is achieved, producing higher final adoption rates.

For networks with a high average node degree ($\bar{k} = 10$, panel b in Figure 11), the picture changes substantially. The optimum shifts to the right creating a monotonically increasing relationship between clustering and adoption at all rewiring levels. This is consistent with the critical mass argument mentioned earlier: in high degree networks, more absolute adopting neighbours are needed to surpass the threshold. However, higher rewiring now consistently produces lower adoption across the full range of clustering values. In high degree networks, rewiring disperses connections that would otherwise contribute to the dense local reinforcement needed to reach critical mass, rather than creating useful bridges to less connected parts of the network.

Moving back to the third row of Figure 10 we see the Snowball strategy produces a different pattern from both the Shotgun and Silver Bullets strategies. The Snowball strategy seeds innovators from a focal node with the highest centrality of complex closeness and expands outward to direct neighbours and the most connected peers (see Section 3.3). This concentrated seeding has the consequence that to achieve a network wide adoption, it relies heavily on having enough reinforcing nodes to trigger a global cascade. Therefore, the average node degree plays a more important role within the Snowball strategy than in the case of the Shotgun and Silver Bullets strategies. For high degree networks (blue lines, $\bar{k} = 10$), the snowball strategy performs substantially better than for low degree networks across the full range of clustering values. The reason for this is that the higher degree of nodes, even a spatially concentrated cluster of innovators, have more potential reinforcing nodes to achieve high final adoption rate. In low degree networks by contrast, the seeded cluster is so sparsely connected to the rest of the network that the cascade almost never reaches the other parts of the network, producing consistently low adoption rates regardless of clustering level.

Across a substantial part of the parameter space, adoption outcomes are bimodally distributed (square shaped), reflecting how the balance between local cascade initiation and access to wide bridges shapes diffusion dynamics. For Shotgun and Silver Bullets seeding, innovators are distributed across the network, such that low clustering makes local cascades difficult to initiate, while successful local initiation almost invariably propagates through wide bridges into a global cascade, producing pronounced all-or-nothing outcomes. For the Snowball strategy, innovators are spatially concentrated within a single neighbourhood, such that high clustering amplifies bimodality: local cascades are readily initiated due to strong local reinforcement, but whether adoption becomes global depends on the presence of sufficiently reinforced wide bridges outward from the seeded cluster, causing adoption to either remain confined or spread network-wide.

5.3 Effect of variance in node degree and communities

The results in the previous section demonstrates how the optimum shifts on the clustering axis due to the dynamics between seeding strategies, innovator density, and node degree. Within this analysis, we controlled as much as possible for modularity and variance node degree by fixing the parameters of communities to 1 and Dekker's power to 0 (for explanation regarding the effect of these parameters see Figure 3. However, when altering these parameters and examining the effect on the optimum when variance in node degree and modularity changes, shows that looking at solely local clustering coefficient as single network metric is not sufficient to represent the optimum between reinforcing nodes and wide bridges.

Figure 12 shows the final adoption rate for the Silver Bullet seeding strategy across networks with varying variance in node degree (panel a) and varying mean local clustering coefficient (panel b). Networks with high variance in node degree, regardless of their clustering coefficient, consistently lead to high final adoption rates. Due to the Silver Bullet strategy seeding people with large node degree as innovators, the critical mass for adoption by connected people increases significantly, reducing the need for reinforcing nodes or wide bridges. Only when variance in node degree decreases substantially, driven by lower Dekker's Power settings, the adoption rates rise start to decline and local clustering becomes necessary to cause final adoption rates to increase. This reveals that in centralised networks, high degree nodes substitute local clustering as the primary driver of cascade propagation. Within this kind of network topologies, implementing realistic seeding strategies becomes much more essential, as people with high node degree are crucial to reach high final adoption rates.

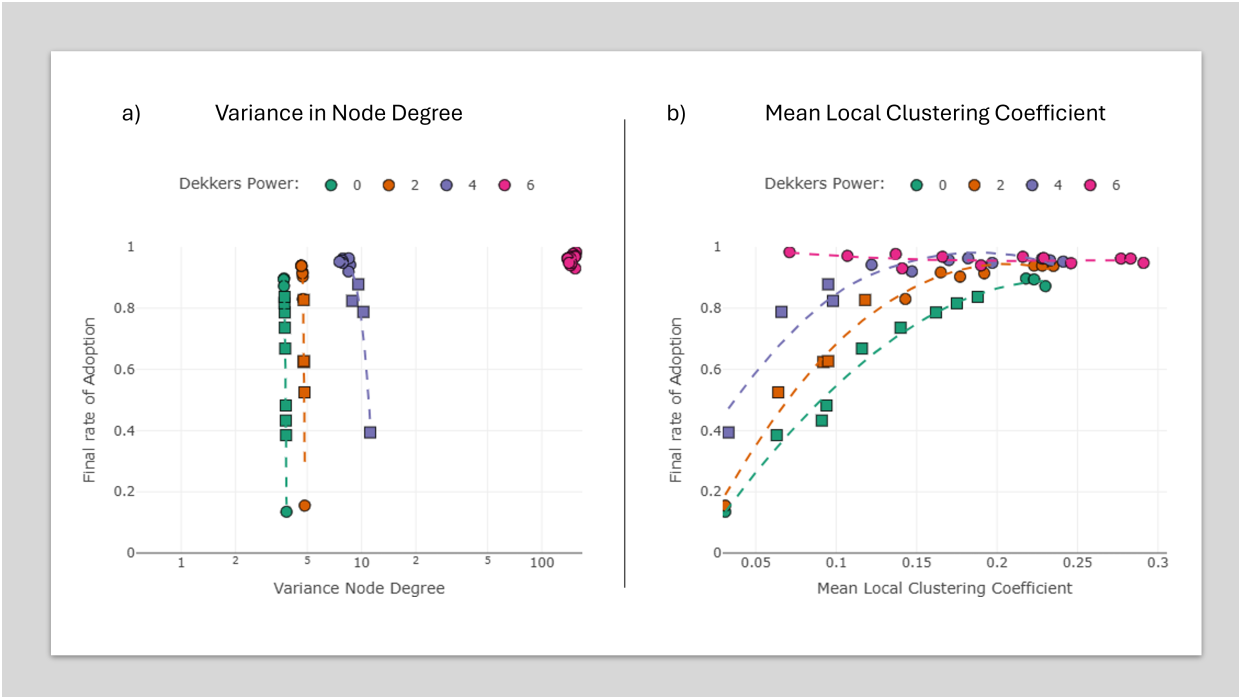

Fig 12. Final adoption rate for the Silver bullet seeding strategy in centralised network topologies. Panel a) shows final adoption rate against variance in node degree, colored by Dekker's Power. Panel b) shows final adoption rate against mean local clustering coefficient, colored by Dekker's Power. Settings: Decision Module = Threshold 0.4, Innovators = 0.1, Node Degree = 10, Communities = All, Rewiring Proportion = 0.2, Clustering Exponent = All. The round shaped markers indicate that across repetitive runs, the adoption outcome is unimodal distributed. Square shaped markers have a bimodal adoption distribution.

The second illustration regarding the insufficiency of local clustering as a single network metric is about the role of predefined communities within the network topology. Figure 13 shows final adoption rate plotted against modularity (panel a) and mean local clustering coefficient (panel a) for networks with one, five, and ten predefined communities. The critical pattern is visible in panel b. For networks with a single predefined community, the relationship between clustering and adoption follows the familiar parabolic trajectory: adoption rises as clustering increases up to a moderate optimum, then slowly declines as for very high clustering cascades get stuck locally due to a lack of wide bridges. As the number of predefined communities increases to five and ten, the optimum follows a bell-curve with a very low optimum. For networks with multiple predefined communities, the constraint for higher final adoption rates is no longer the local clustering structure within communities but the number of wide bridges between the local neighbourhoods within the network. Panels b and c of Figure 13 show how modularity and variance in the local clustering coefficient are better predictors of when there are sufficient wide bridges that can trigger high final adoption rates. In panel b, modularity indicates the strength of segregation between communities. Within single community networks, higher modularity means that more local clustering is combined with sufficient pre-existing wide bridges. For networks with five or ten communities, high modularity means the lack of wide bridges and that communities are very clearly segregated. Sufficient wide bridges are best detected by looking in the variance of the local clustering coefficient. Nodes with low local clustering coefficients are structurally positioned between communities, with neighbours drawn from different groups who share few mutual connections, making them the wide bridges between communities. Higher variance in local clustering therefore signals the co-existence of densely connected reinforcing nodes and sparsely connected bridge nodes.

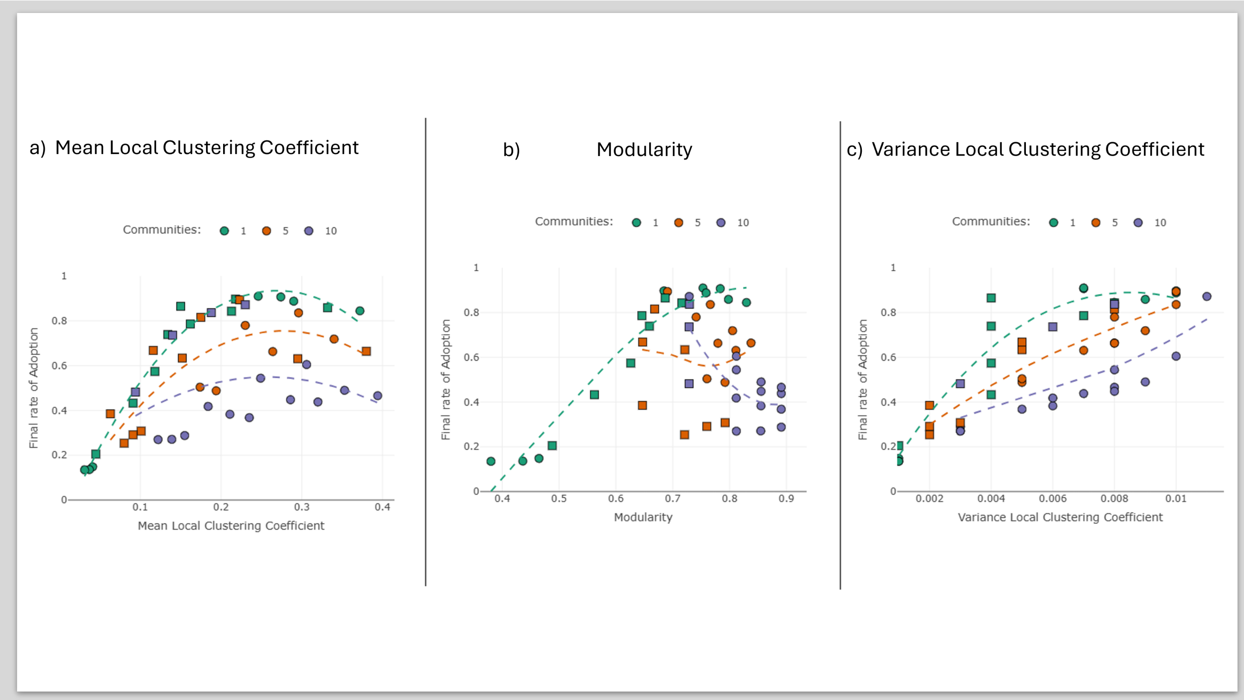

Fig 13. Overview of how final adoption rate is sensitive to networks that differ in terms of Mean Local Clustering Coefficient (Panel a), Modularity (Panel B) and Variance Local Clustering Coefficient. Colors indicate number of preset communities. Other settings are: Decision Module = Threshold = 0.4, Innovators = 0.1, Seeding Strategy = Silver Bullets, Node Degree = 10, Dekker's Power = 0, Rewiring Proportion = All. The round shaped markers indicate that across repetitive runs, the adoption outcome is unimodal distributed. Square shaped markers have a bimodal adoption distribution.

6 Discussion

Through a systematic full factorial analysis, we have demonstrated that the final adoption rate peaks based on the optimum between the required reinforcing nodes around the initial innovators and the wide bridging connections between local neighborhoods. The results deliver four interrelated contributions to this question, concluding with five practical implications for researchers designing sensitivity analyses in larger ABMs.

6.1 Adoption optimum based on the calibration of threshold values and innovator density.

The threshold value and the innovator density together calibrate the balance between the local and global phases of a complex contagion cascade. When the threshold is low or innovators are numerous, local critical mass is reached without requiring a large number of reinforcing nodes, and the optimum shifts toward lower clustering where wide bridges are more abundant. When the innovator density decreases, more reinforcing nodes are required to initiate a local cascade, pushing the parabolic adoption optimum toward higher clustering. This mechanism is consistent with the theoretical arguments of complex contagion by Centola and Macy [46] and Watts [30].

6.2 Structural components shift the optimum independently of seeding or threshold values.

Variance in node degree and modularity each independently alter the adoption dynamics in ways that cannot be detected by examining mean local clustering alone. In centralised networks with high variance in node degree, hub nodes substitute for local clustering as the primary driver of global cascade propagation, rendering the optimum in clustering largely invisible. In multi-community networks, the same level of mean clustering that enables global cascades in a single-community network becomes a barrier to inter-community diffusion as modularity increases. These findings directly extend the concern about the difficulty of disentangling the confounding effects of network properties as mentioned by [35]. The results highlight the importance of performing a Full Factorial analysis by showing that a continuous, multi-dimensional parameter sweep can make those confounding relationships transparent and quantifiable.

6.3 Use mean adoption rates with care

Beyond shifting optima, the results showed that variation in final adoption rates across repetitive runs are dominated by bimodal outcome distributions. For a substantial part of the parameter space, repeated runs on identical network configurations yield either near-zero adoption, when a local cascade fails to escape the initial neighbourhood, or near-complete adoption once the cascade successfully bridges to the wider network. In these cases, the mean final adoption rate approximates the probability that a global cascade occurs under the given configuration. This implies that smooth response curves based on averaged outcomes can obscure the underlying all-or-nothing dynamics of threshold-based complex contagion. Network topologies that appear similar based on average adoption may therefore differ fundamentally in their reliability. Some configurations produce unimodal adoption outcomes centred around the mean, while others have more volatility in the final adoption rates in which small alteration in seeding or network structure determines success or failure. These bimodal distributions highlights the probabilistic nature of behavior adoption (i.e. social tipping) which is shaped by network structure.

6.4 Too much emphasis on finding the 'optimal seeding strategy'.

Conclusions about the optimal seeding strategy are always conditional based on the settings for threshold, innovator density, degree variance, and modularity. The dominant approach in the literature benchmarks seeding strategies across networks [29,32], or documents that structural properties matter while acknowledging that confounding prevents clean attribution [35]. Neither approach directly asks how the optimum moves as components are jointly varied. A sensitivity analysis oriented around the *displacement of the optimum* makes these conditionalities explicit and therefore produces conclusions that are more transparently and generalisable.

6.5 How to analyse the impact of network topology in largers abms with a full factorial sensitivity analysis.

Based on the three formulated findings above, we articulate the importance of reframing sensitivity analysis of network topology from a search for a single optimal configuration to a mapping of how the optimum moves across a multi-dimensional parameter space. Therefore, we propose the following guidelines for designing the sensitivity analysis of agent-based network-based models, especially for researchers who embed peer influence networks within larger policy models.

1. Reflect on whether the implemented decision-module in the model aligns with the empirical behavior of the studied population. The operationalion of the decision-module, for example the reversibility of adoption, highly affects the presence of model output sensitivity to network structural components.

2. For the given seeding strategy, whether it is exogeneous or endogeneously integrated in the model, start by altering the threshold values and innovator density jointly to identify the intermediate parameter window in which the model is sensitive.

3. Inspect and report the distribution of outcomes across repetitions, rather than relying solely on mean adoption rates. In threshold-based contagion models, bimodal outcome distributions are common, in which case mean adoption reflects the probability of a global cascade rather than a typical adoption level.

4. Next, decide based on the selected case which part of the structural components of the network has the highest uncertainty and adjust the sensitivity analysis accordingly. So, if, for example, the network for the case study is about the spread of behavioural adoption across multiple neighbourhoods in a city. The experimental design of the sensitivity analysis should mainly focus on varying the number of communities, rewiring, and average node degree for analysing the impact of wide bridges.

5. Lastly, the variance in node degree and modularity should be reported and varied alongside mean clustering, rather than treated as fixed background properties, because they may explain the observed non sensitivity to clustering. Studies on local energy communities confirm that clustering and modularity are empirically relevant for participation dynamics [10, 47], further motivating the need for this kind of structural disaggregation.

.

6.6 Network topology and Social Tipping Points

The results indicate that the volatility in final adoption rate is a structural property of threshold-based contagion dynamics. Even under the most stylized modelling assumptions (i.e. two behavioral states, no reversibility, homogeneous thesholds values, homogeneous connection weights), the critical mass required to trigger a self-sustaining cascade of behavioral change varies widely due to the configuration between seedings strategies, innovator density and network topology.

This finding has direct implications for the growing call to endogenously integrate social tipping dynamics within larger integrated assessment models [11]. Before policy-relevant inference can be drawn from such models, a thorough sensitivity analysis across the joint distribution of threshold values and network parameters is essential. Social Tipping points may therefore be better understood as clarifying phenomena used in scenario building, than as predictive targets. We therefore recommend that researchers embedding peer-influence networks in larger policy models adopt a network-generating approach that makes structural uncertainty explicit. Rather than running a scenario analysis with two or three stylised topologies, networks with clustering, degree variance, and modularity should be tested as independent continuous parameters. In this light, we would like to emphasise that the relevant research questions to be asked are not where the tipping point lies or how policy might cause tipping, but why acceleration of change occurs or fails to under specific configurations of infrastructure, institutions, and social structure.

6.7 Limitations

A limitation of the present study is that the model deliberately avoids the heterogeneity of threshold values and directional weighted networks, which are likely features of empirical peer-influence networks [3, 36]. Future work should examine whether the optimum-shift patterns identified here are robust to the introduction of threshold heterogeneity, and whether the TENTASS network-generating model can be extended to accommodate weighted or directed ties without losing the independence of its structural parameters.

7 Conclusion

To address the uncertainty around how network topology and seeding strategies jointly shape adoption outcomes under peer influence, we developed the TENTASS model: an agent-based simulation that independently controls local clustering, variance in node degree, and average node degree as continuous variables. Through a systematic full factorial analysis, we demonstrated that final adoption rates peak at an optimum level of clustering that balances local reinforcement through reinforcing nodes against global reach through wide bridges, and that this optimum shifts depending on threshold values, innovator density, and average node degree. Variance in node degree and modularity are independent structural drivers that can flatten or eliminate this parabolic relationship. For a substantial part of the parameter space, adoption outcomes are bimodal distributed, suggesting that complex contagion can be characterised as a probabilistic event whose likelihood is shaped by network configuration rather than a deterministic threshold. These findings motivate a practical guideline for sensitivity analysis in larger ABMs: verify that threshold and innovator settings fall within the structurally sensitive window, report and vary degree variance and modularity alongside mean clustering, and co-vary seeding strategy with network structure rather than optimising them independently.

Acknowledgments

Appendix: Model parameters, variables and network structural metrics

Table 2. Overview of all symbols, parameters, network structural metrics, equation-level variables, and the output variable used in the TENTASS model. Organised into five sections: (i) Input parameters, (ii) Output parameters, (iii) Agent-level variables, (iv) Model variables, (v) network structural metrics

Symbol	Full name	Definition	Role
(i) Model input parameters			
N	Total population	Number of agents in the network	Fixed structural baseline
$\bar{k}$	Average node degree	Mean number of connections per agent: $\bar{k} = \frac{1}{N}\sum_{i=1}^{N} k_i$	Determines the total number of connections in the network
C	Clustering exponent	Controls probability of within-community connections based on identity distance (Eq. 3). Higher C produces higher local clustering	Primary input driver of mean local clustering coefficient
R	Rewiring proportion	Proportion of connections rewired irrespective of community membership. Higher R reduces clustering and introduces wide bridges	Primary input driver of wide bridge formation
Q	Dekker's power	Exponent controlling preferential attachment during rewiring (Eq. 4). Higher Q creates hub nodes with high degree variance	Primary input driver of variance in node degree

Continued on next page

Table 2 continued from previous page

Symbol	Full name	Definition	Role
G	Number of communities	Number of predefined communities agents are assigned to	Primary input driver of network modularity
S	Seeding strategy	Method for selecting initial innovators: Shotgun (random), Silver Bullets (highest k_i), Snowball (highest complex closeness centrality c_x)	Determines spatial distribution of innovators in the network
ρ	Innovator density	Proportion of agents designated as initial innovators ($b = 1$)	Calibrates local critical mass requirements
D	Decision-making module	Rule governing adoption: Threshold (irreversible, Eq. 1) or Probabilistic (reversible, Eq. 2)	'Stickiness' of behavior important requirement for network sensitivity
T	Threshold	Fraction of adopting peers required to trigger adoption under the threshold module	Calibrates local critical mass requirements to trigger cascade
ϵ_1, ϵ_2	Smoothing constants	Small positive constants set to 10^{-6} preventing division by zero in the probabilistic module while keeping stochastic noise negligible	Numerical stability constants in probabilistic decision module (Eq. 2)
(ii) Output variable			
FAR	Final adoption rate	Proportion of agents holding $b = 1$ at simulation end. For threshold module: share at timestep when no further adoption occurs. For probabilistic module: share when 95% or 5% stopping condition is met	Primary outcome variable across all simulation runs
(iii) Agent attributes			
b	Behaviour attribute	Binary state of each agent: $b \in \{0, 1\}$, where $b = 0$ is current behaviour and $b = 1$ is the alternative sustainable behaviour	Core state variable tracking adoption status of each agent
I	Identity value	Unique integer assigned to each agent at initialisation	Determines agent ordering within communities and clustering structure (Eq. 3)
k_i	Node degree	Number of connections of agent i	Used for Silver Bullets seeding strategy selection and degree variance calculation
c_x	Complex closeness centrality	$c_x = \frac{1}{\sum_{y \neq x}(w_{x \to y})}$, where $w_{x \to y}$ is the complex edge weight (Eq. 5) [29]	Used for Snowball seeding strategy to identify the focal innovator node
(iv) Model variables			

Continued on next page

Table 2 continued from previous page

Symbol	Full name	Definition	Role
E_{xy}	Edge indicator	Binary variable indicating whether a connection exists between agents x and y: $E_{xy} \in \{0, 1\}$	Used in network generation equations (Eq. 3, Eq. 4)
F	Total peers	Total number of connected peers of a focal agent	Denominator in threshold and probabilistic decision module equations
$F_{b_{t-1}=1}$	Adopting peers	Number of peers who held behaviour $b = 1$ at the previous timestep	Numerator in threshold decision module (Eq. 1)
o_{xy}	Shared neighbours	Number of nodes connected to both x and y	Component of complex edge weight $w_{x \to y}$ (Eq. 5)
r_{xy}	Reinforcing nodes	Number of nodes connected to y but not x that share at least one connection with a neighbour of x	Component of complex edge weight capturing indirect reinforcing influence (Eq. 5)
$w_{x \to y}$	Complex edge weight	$w_{x \to y} = \frac{1}{1+o_{xy}+r_{xy}}$, weighting directed shortest paths by reinforcing influence of shared connections [29]	Core measure of directional reinforcing influence between agents; basis for complex closeness centrality
(v) Network structural metrics			
MLC	Mean local clustering coefficient	$\text{MLC} = \frac{1}{N} \sum_i C_i$ [40, 48]	Primary measure of reinforcing node density; high MLC means adoption signals arrive through mutually connected neighbours
VD	Variance in node degree	$\text{VD} = \frac{1}{N} \sum_{i=1}^{N} (k_i - \bar{k})^2$ [44]	Captures network centralisation; high VD signals hub nodes that can substitute for local clustering as cascade driver
MOD	Modularity (Louvain)	$Q = \frac{1}{2m} \sum_{ij} \left[A_{ij} - \frac{k_i k_j}{2m} \right] \delta(c_i, c_j)$ [49, 50]	Captures structural barriers to inter-community diffusion; high modularity means wide bridges between communities are scarce
VLC	Variance in local clustering coefficient	$\text{VLC} = \frac{1}{N} \sum_{i=1}^{N} (C_i - \text{MLC})^2$	Signals co-existence of densely clustered reinforcing nodes and sparsely connected bridge nodes
MPL	Mean path length	$\text{MPL} = \frac{1}{N(N-1)} \sum_{i \neq j} l_{ij}$ [40, 48]	Inversely related to global speed of cascade spread; high MPL indicates fragmented or locally clustered structure

Continued on next page

Table 2 continued from previous page

Symbol	Full name	Definition	Role
MCPL	Mean complex path length	Mean shortest-path length on the complex-weighted directed graph using $w_{x \to y}$ as edge weights (Eq. 5) [29]	Low MCPL indicates densely reinforced directed paths; high MCPL indicates paths through structurally weak wide bridges
GCC	Global clustering coefficient	Ratio of closed triplets to all triplets in the network [40, 48]	Alternative clustering measure weighting nodes by degree rather than averaging uniformly

References

1. Milkoreit M. Social tipping points everywhere?—Patterns and risks of overuse. Wiley Interdisciplinary Reviews: Climate Change. 2023;14(2):e813.

2. Perlaviciute G, Steg L, Sovacool BK. A perspective on the human dimensions of a transition to net-zero energy systems. Energy and Climate Change. 2021;2:100042.

3. Wolske KS, Gillingham KT, Schultz PW. Peer influence on household energy behaviours. Nature Energy. 2020;5(3):202–212.

4. Alkemade F, de Bruin B, El-Feiaz A, Pasimeni F, Niamir L, Wade R. Social tipping dynamics in the energy system. Earth System Dynamics. 2024;15(2):485–500.

5. Graziano M, Gillingham K. Spatial patterns of solar photovoltaic system adoption: the influence of neighbors and the built environment. Journal of Economic Geography. 2015;15(4):815–839.

6. Grinblatt M, Keloharju M, Ikäheimo S. Social influence and consumption: Evidence from the automobile purchases of neighbors. The review of Economics and Statistics. 2008;90(4):735–753.

7. Allcott H. Social norms and energy conservation. Journal of public Economics. 2011;95(9-10):1082–1095.

8. Bergquist M, Nilsson A. I saw the sign: Promoting energy conservation via normative prompts. Journal of Environmental Psychology. 2016;46:23–31.

9. Selvakkumaran S, Ahlgren EO. Determining the factors of household energy transitions: A multi-domain study. Technology in Society. 2019;57:54–75.

10. Goedkoop F, Dijkstra J, Flache A. A social network perspective on involvement in community energy initiatives: The role of direct and extended social ties to initiators. Energy Policy. 2022;171:113260.

11. Niamir L, Creutzig F. Closing the gap: Integrating behavioral and social dynamics through a modular modelling framework for low-energy demand pathways. Energy Research & Social Science. 2025;122:103988.

12. Erickson BH. The Relational Basis of Attitudes. American Journal of Sociology. 1988;93(6):1241–1278. doi:10.1086/228906.

13. Marsden PV, Friedkin NE. Network Studies of Social Influence. Sociological Methods & Research. 1993;22(1):127–151. doi:10.1177/0049124193022001006.

14. Friedkin NE. A Structural Theory of Social Influence. Chicago: University of Chicago Press; 1998.

15. Nolan JM, Schultz PW, Cialdini RB, Goldstein NJ, Griskevicius V. Normative social influence is underdetected. Personality and social psychology bulletin. 2008;34(7):913–923.

16. Kossinets G. Effects of missing data in social networks. Social networks. 2006;28(3):247–268.

17. Wang DJ, Shi X, McFarland DA, Leskovec J. Measurement error in network data: A re-classification. Social Networks. 2012;34(4):396–409.

18. Konc T, Savin I, Van Den Bergh JC. The social multiplier of environmental policy: Application to carbon taxation. Journal of Environmental Economics and Management. 2021;105:102396.

19. Lackner T, Fierro LE, Mellacher P. Opinion dynamics meet agent-based climate economics: An integrated analysis of carbon taxation. Journal of Economic Behavior & Organization. 2025;229:106816.

20. Li Y, Zhang D, Pagán JA. Social norms and the consumption of fruits and vegetables across New York City neighborhoods. Journal of urban health. 2016;93(2):244–255.

21. Chappin EJ, Afman MR. An agent-based model of transitions in consumer lighting: Policy impacts from the EU phase-out of incandescents. Environmental Innovation and Societal Transitions. 2013;7:16–36.

22. Rai V, Robinson SA. Agent-based modeling of energy technology adoption: Empirical integration of social, behavioral, economic, and environmental factors. Environmental Modelling & Software. 2015;70:163–177.

23. Du H, Han Q, de Vries B. Modelling energy-efficient renovation adoption and diffusion process for households: A review and a way forward. Sustainable Cities and Society. 2022;77:103560.

24. Castro J, Drews S, Exadaktylos F, Foramitti J, Klein F, Konc T, et al. A review of agent-based modeling of climate-energy policy. Wiley Interdisciplinary Reviews: Climate Change. 2020;11(4):e647.

25. McCoy D, Lyons S. Consumer preferences and the influence of networks in electric vehicle diffusion: An agent-based microsimulation in Ireland. Energy Research & Social Science. 2014;3:89–101.

26. Moglia M, Podkalicka A, McGregor J. An Agent-Based Model of Residential Energy Efficiency Adoption. Journal of Artificial Societies and Social Simulation. 2018;21(3):3. doi:10.18564/jasss.3729.

27. Granovetter M. Threshold models of collective behavior. American journal of sociology. 1978;83(6):1420–1443.

28. Centola D. How behavior spreads: The science of complex contagions. vol. 3. Princeton University Press Princeton, NJ; 2018.

29. Guilbeault D, Centola D. Topological measures for identifying and predicting the spread of complex contagions. Nature communications. 2021;12(1):4430.

30. Watts DJ. A simple model of global cascades on random networks. Proceedings of the National Academy of Sciences. 2002;99(9):5766–5771.

31. Singh P, Sreenivasan S, Szymanski BK, Korniss G. Threshold-limited spreading in social networks with multiple initiators. Scientific reports. 2013;3(1):2330.

32. Montes F, Jaramillo AM, Meisel JD, Diaz-Guilera A, Valdivia JA, Sarmiento OL, et al. Benchmarking seeding strategies for spreading processes in social networks: an interplay between influencers, topologies and sizes. Scientific Reports. 2020;10(1):3666.

33. Hackett A, Melnik S, Gleeson JP. Cascades on a class of clustered random networks. Physical Review E—Statistical, Nonlinear, and Soft Matter Physics. 2011;83(5):056107.

34. Badham J, Kee F, Hunter RF. Simulating network intervention strategies: Implications for adoption of behaviour. Network Science. 2018;6(2):265–280.

35. Badham J, Kee F, Hunter RF. Network structure influence on simulated network interventions for behaviour change. Social Networks. 2021;64:55–62.

36. Valente TW, Vega Yon GG. Diffusion/contagion processes on social networks. Health Education & Behavior. 2020;47(2):235–248.

37. Centola D. The spread of behavior in an online social network experiment. science. 2010;329(5996):1194–1197.

38. Dodds PS, Watts DJ. Universal behavior in a generalized model of contagion. Physical review letters. 2004;92(21):218701.

39. Ugander J, Backstrom L, Marlow C, Kleinberg J. Structural diversity in social contagion. Proceedings of the national academy of sciences. 2012;109(16):5962–5966.

40. Watts DJ, Strogatz SH. Collective dynamics of 'small-world'networks. nature. 1998;393(6684):440–442.

41. Granovetter M, Soong R. Threshold models of diffusion and collective behavior. Journal of Mathematical sociology. 1983;9(3):165–179.

42. Kleinberg JM. Navigation in a small world. Nature. 2000;406(6798):845–845.

43. Dekker A. Realistic social networks for simulation using network rewiring. In: International congress on modelling and simulation; 2007. p. 677–683.

44. Albert R, Barabási AL. Statistical mechanics of complex networks. Reviews of modern physics. 2002;74(1):47.

45. ANONYMOUS. Make uncertainty in Social Tipping models explicit! A systematic sensitivity analysis of network topology in peer-influence models; 2026. `https://doubleblindresearchoutcome.shinyapps.io/TENTASS/`.

46. Centola D, Macy M. Complex contagions and the weakness of long ties. American journal of Sociology. 2007;113(3):702–734.

47. Geskus S, Punt MB, Bauwens T, Corten R, Frenken K. Does social capital foster renewable energy cooperatives? Journal of Economic Geography. 2024;24(6):887–905.

48. Newman MEJ. Networks: An Introduction. Oxford: Oxford University Press; 2010.

49. Blondel VD, Guillaume JL, Lambiotte R, Lefebvre E. Fast unfolding of communities in large networks. Journal of statistical mechanics: theory and experiment. 2008;2008(10):P10008.

50. Newman MEJ. Modularity and community structure in networks. Proceedings of the National Academy of Sciences. 2006;103(23):8577–8582. doi:10.1073/pnas.0601602103.